ARTICLE

doi:10.1038/nature11088

# Peroxiredoxins are conserved markers of circadian rhythms

Rachel S. Edgar[1]*, Edward W. Green[2]*, Yuwei Zhao[3]*, Gerben van Ooijen[4]*, Maria Olmedo[5]*, Ximing Qin[3], Yao Xu[3], Min Pan[6], Utham K. Valekunja[1], Kevin A. Feeney[1], Elizabeth S. Maywood[7], Michael H. Hastings[7], Nitin S. Baliga[6], Martha Merrow[5], Andrew J. Millar[4,8], Carl H. Johnson[3], Charalambos P. Kyriacou[2], John S. O'Neill[1] & Akhilesh B. Reddy[1]

**Cellular life emerged ~3.7 billion years ago. With scant exception, terrestrial organisms have evolved under predictable daily cycles owing to the Earth's rotation. The advantage conferred on organisms that anticipate such environmental cycles has driven the evolution of endogenous circadian rhythms that tune internal physiology to external conditions. The molecular phylogeny of mechanisms driving these rhythms has been difficult to dissect because identified clock genes and proteins are not conserved across the domains of life: Bacteria, Archaea and Eukaryota. Here we show that oxidation–reduction cycles of peroxiredoxin proteins constitute a universal marker for circadian rhythms in all domains of life, by characterizing their oscillations in a variety of model organisms. Furthermore, we explore the interconnectivity between these metabolic cycles and transcription–translation feedback loops of the clockwork in each system. Our results suggest an intimate co-evolution of cellular timekeeping with redox homeostatic mechanisms after the Great Oxidation Event ~2.5 billion years ago.**

Circadian rhythms are considered to be a feature of almost all living cells. When isolated from external stimuli, organisms exhibit self-sustained cycles in behaviour, physiology and metabolism, with a period of approximately 24 h[1]. Circadian clocks afford competitive selective advantages that have been observed experimentally[2,3], and disturbance of circadian timing in humans, as seen in rotational shift work and jet lag, carries long-term health costs[4]. For all organisms in which the molecular timing mechanism has been investigated, a common model has arisen, namely a transcription–translation feedback loop (TTFL). TTFL components are not, however, shared between organisms. For example, the cyanobacterial clock is modelled around three proteins: KaiA, B and C. In the fungus *Neurospora crassa*, a loop involving the protein FREQUENCY (FRQ) and the WHITE COLLAR (WC) complex is thought to drive cellular rhythms, whereas the plant TTFL involves elements including TOC1 and CCA1 (refs 1, 5). Furthermore, although some multicellular organisms such as *Drosophila* and humans possess homologous components (for example, the Period proteins), their functions seem to differ between organisms[6–8]. Therefore, across phylogenetic kingdoms, there are apparently no common 'clock' components, suggesting that daily timekeeping evolved independently within different lineages. The converse, however, could equally be true, and the primary premise of this study was therefore to test the hypothesis that circadian clocks may instead have a common ancestry.

## Conservation of peroxiredoxin in circadian systems

Recent studies show that the oxidation state of highly conserved peroxiredoxin (PRX) proteins exhibit circadian oscillations in cells from humans, mice and marine algae[9,10], probably reflecting an endogenous rhythm in the generation of reactive oxygen species (ROS)[10]. Because virtually all living organisms possess peroxiredoxins[11], we proposed that this marker for circadian rhythms in metabolism may be functionally conserved across all three phylogenetic domains: Archaea, Bacteria and Eukaryota. Peroxiredoxins are peroxidases, the activity of which is dependent on the oxidation of a key 'peroxidatic' cysteine residue ($C_p$) in the active site, that is absolutely conserved, as are neighbouring proline and threonine/serine residues: conforming to a PXXX(T/S)XX$C_p$ consensus[12]. Crucially, the catalytic cysteine can become over- or hyperoxidized (PRX-$SO_{2/3}$), rendering the peroxiredoxin catalytically inactive, but able to participate in ROS signalling and chaperone activity[13]. Once overoxidized, peroxiredoxin can be recycled by sulphiredoxin.

We previously characterized circadian cycles of peroxiredoxin oxidation using antiserum directed against the oxidized active site, which recognizes both over- (PRX-$SO_2$) and hyper- (PRX-$SO_3$) oxidized forms[9,10,14]. To determine whether this antiserum (raised against an oxidized DFTFVCPTEI peptide) could be used to assay over-/hyperoxidation in diverse species, we performed several sequence alignments to compare peroxiredoxin protein sequences across a variety of circadian model organisms. This revealed a remarkable degree of conservation across all phylogenetic domains, especially within the active site (Fig. 1a, Supplementary Fig. 1 and Supplementary Tables 1–7). Even when we examined the structure of HyrA, the most distantly related peroxiredoxin orthologue in the archaeon *Halobacterium salinarum* sp. NRC-1, we found that amino acid substitutions would not perturb the geometry of the active site (Fig. 1b). Together, these findings suggested that the same antiserum could be used to probe oxidation rhythms in potentially any organism expressing a peroxiredoxin protein. This was confirmed by gene knockout and peroxide treatment in several representative organisms (Supplementary Figs 3 and 7–9).

[1]Department of Clinical Neurosciences, University of Cambridge Metabolic Research Laboratories, NIHR Biomedical Research Centre, Institute of Metabolic Science, University of Cambridge, Addenbrooke's Hospital, Cambridge CB2 0QQ, UK. [2]Department of Genetics, University of Leicester, Leicester LE1 7RH, UK. [3]Department of Biological Sciences, Vanderbilt University, Nashville, Tennessee 37235-1634, USA. [4]Synthetic and Systems Biology (SynthSys), Mayfield Road, Edinburgh EH9 3JD, UK. [5]Department of Molecular Chronobiology, Center for Life Sciences, University of Groningen, 9700 CC Groningen, The Netherlands. [6]Institute for Systems Biology, 401 Terry Avenue North, Seattle, Washington 98109, USA. [7]MRC Laboratory of Molecular Biology, Hills Road, Cambridge CB2 2QH, UK. [8]School of Biological Sciences, University of Edinburgh, Mayfield Road, Edinburgh EH9 3JR, UK.
*These authors contributed equally to this work.



©2012 Macmillan Publishers Limited. All rights reserved

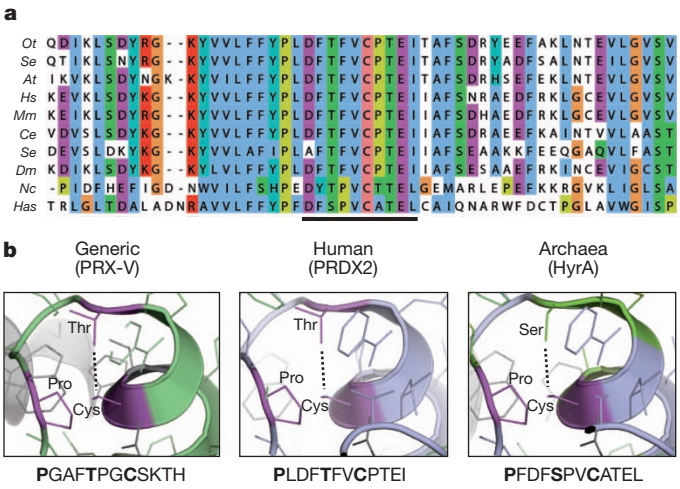


**Figure 1 | The peroxiredoxin active site is highly conserved in all domains of life.** **a**, Multiple sequence alignment showing peroxiredoxin amino acid sequences. The highly conserved active site is underlined. Representatives shown from Eukaryota (*At*, *A. thaliana*; *Ce*, *Caenorhabditis elegans*; *Dm*, *D. melanogaster*; *Hs*, *Homo sapiens*; *Mm*, *M. musculus*; *Nc*, *N. crassa*; *Ot*, *O. tauri*; *Sc*, *S. cerevisiae*), Bacteria (*Se*, *S. elongatus* sp. PCC7942) and Archaea (*Has*, *H. salinarum* sp. NRC-1). **b**, Critical residues in the active site of 2-Cys peroxiredoxins (in bold) are conserved in all organisms. Structures were derived from human PRX-V (Protein Data Bank (PDB) accession 1HD2)[47] and human PRDX2 (PDB accession 1QMV)[48], and modified with PyMOL to show the predicted structure for archaeal peroxiredoxin (HyrA, GenBank accession NP_280562.1).

## Peroxiredoxin rhythms in eukaryotes

Using the PRX-$SO_{2/3}$ antiserum, we first examined circadian time courses from a range of eukaryotes under constant conditions (that is, in the absence of external timing cues). In mice, PRX-$SO_{2/3}$ and total PRX1 exhibited a daily cycle in liver tissue and also in the central pacemaker, the suprachiasmatic nuclei (SCN) of the hypothalamus (Fig. 2a). Interestingly, between the two tissues, peroxiredoxin oxidation rhythms were in distinct, and different, phase relationships with respect to total PRX1 and BMAL1 protein, suggesting a difference between brain and peripheral tissue (Fig. 2a), as observed previously for other clock components[15].

To extend these findings beyond vertebrates, we examined peroxiredoxin rhythms in the fruitfly *Drosophila melanogaster*. We pooled whole heads from insects maintained in constant darkness over two circadian cycles after they had been stably entrained to 12 h light, 12 h dark cycles. Again, circadian oscillations in PRX-$SO_{2/3}$ immunoreactivity were observed, as well as in the clock protein Timeless (TIM) (Fig. 2b). Similarly, seedlings from the plant *Arabidopsis thaliana* exhibited robust PRX-$SO_{2/3}$ oscillations in free-running conditions of constant light, which were also seen in the filamentous fungus *Neurospora crassa*—another well-characterized clock model system (Fig. 2c and Supplementary Fig. 2). Therefore, just as in tissue from 'complex' vertebrates, this range of 'simpler' eukaryotic systems had robust peroxiredoxin oxidation cycles, with peaks tending to occur around anticipated dawn.

## Peroxiredoxin rhythms in prokaryotes

Having observed ~24 h peroxiredoxin oxidation rhythms in organisms with nucleated cells, we next sought to examine representative prokaryotes from each major domain—Bacteria and Archaea.

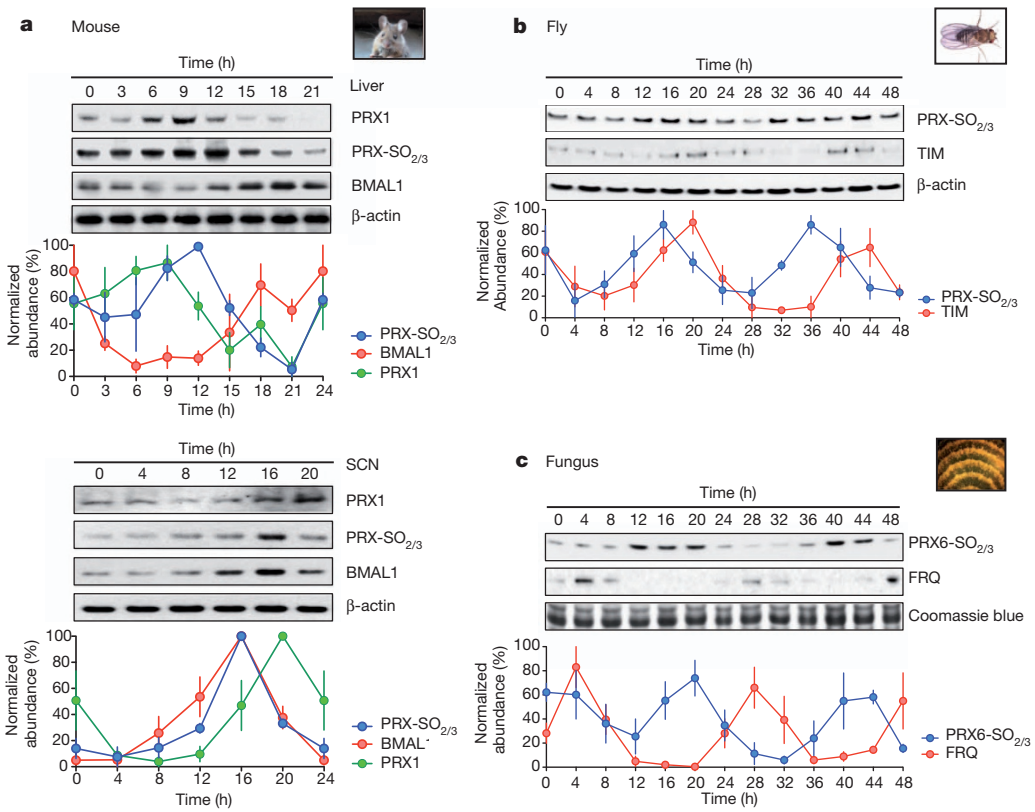


**Figure 2 | Peroxiredoxin oxidation cycles are conserved in eukaryotic models of the circadian clock.** **a**–**c**, Representative immunoblots probed for oxidized/hyperoxidized 2-Cys peroxiredoxin (PRX-$SO_{2/3}$ or PRX6-$SO_{2/3}$) are shown for mouse (*Mus musculus*; **a**), fruitfly (*D. melanogaster*; **b**), and fungus (*N. crassa*; **c**). For each model system, the organism was sampled under free-running conditions. Loading controls show either β-actin immunoblots or Coomassie blue-stained gels loaded with identical samples used for immunoblotting. Immunoblot quantification by densitometry is shown below each panel (mean ± s.e.m.) for $n = 3$ biological replicates. See Supplementary Fig. 2 for plant rhythms, and Supplementary Table 9 for cycle period estimates (by harmonic regression) and detailed statistics (by ANOVA).



©2012 Macmillan Publishers Limited. All rights reserved

For bacteria, we used the best characterized prokaryotic clock model system, *Synechococcus elongatus* sp. PCC7942 (ref. 16). The major proteins involved in the cyanobacterial clockwork are encoded by the *KaiABC* cluster from which, remarkably, circadian oscillations of phosphorylation can be reconstituted *in vitro*[17]. However, because all three Kai proteins are expressed together in only a small number of bacterial species, and in no known archaea[18], this system cannot represent a general prokaryotic clock mechanism. We postulated that, regardless of the timekeeping mechanism, the peroxiredoxin oxidation cycles we observe reflect an absolutely conserved rhythmic cellular output. We tested this by assaying PRX-$SO_{2/3}$ under free-running conditions (constant light) for 48 h, and observed cycles of cyanobacterial peroxiredoxin oxidation, peaking later than phosphorylated KaiC (Fig. 3a).

Furthermore, we extended our studies to the third phylogenetic domain, Archaea, assaying rhythms of peroxiredoxin oxidation in *H. salinarum* sp. NRC-1. Although no clock mechanisms have been identified for any archaeon, diurnal transcriptional rhythms were recently observed in *H. salinarum*[19], and it thus represents an ideal platform to test whether peroxiredoxin oxidation constitutes a universal marker for cellular rhythms. After entraining the archaea for three cycles in 12 h light, 12 h dark cycles, we placed them into constant light at constant temperature. We observed robust, high amplitude circadian oscillations of PRX-$SO_{2/3}$ for three cycles (Fig. 3b). Together, our findings in evolutionarily diverse prokaryotes provide compelling evidence that rhythmic peroxiredoxin oxidation is a conserved circadian marker across phylogenetic domains.

## Relations between peroxiredoxin cycles and TTFLs

In all circadian model systems, the proposed clock mechanism revolves around a TTFL[5,20,21]. How the metabolic rhythms observable through peroxiredoxin oxidation relate to, and interact with, the known transcriptional clockwork in different organisms is unclear. Again, we used several model organisms, with available 'clock' mutants, to address this question.

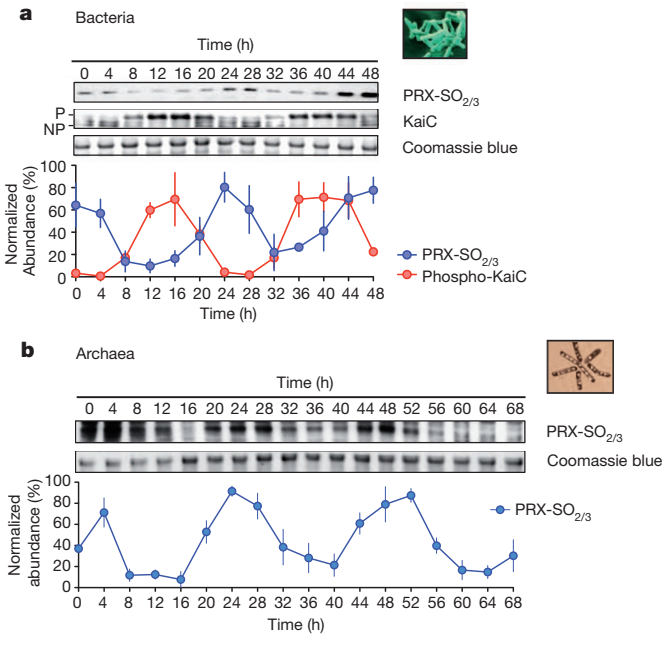


**Figure 3 | Peroxiredoxin oxidation cycles are conserved in prokaryotic models of the circadian clock.** **a**, **b**, Representative immunoblots probed for oxidized/hyperoxidized 2-Cys peroxiredoxin (PRX-$SO_{2/3}$) are shown for bacteria (*S. elongatus* sp. PCC7942; **a**), and archaea (*H. salinarum* sp. NRC-1; **b**). Before sampling under free-running conditions (constant light), cyanobacteria were synchronized with a 12 h dark pulse, whereas archaea were stably entrained to 12 h light, 12 h dark cycles. Loading controls show Coomassie blue-stained gels loaded with identical samples used for immunoblotting. Immunoblot quantification by densitometry is shown below each panel (mean ± s.e.m.) for $n = 3$ biological replicates. See Supplementary Table 9 for cycle period estimates and detailed statistics. P, phosphorylated KaiC; NP, non-phosphorylated KaiC.

The *Drosophila* transcriptional clockwork is structurally similar to the mammalian TTFL, although there are some important differences[22]. In flies, Clock and Cycle (orthologous to mammalian BMAL1, also known as ARNTL) comprise the positive limb, driving oscillatory expression of Period (PER) and Timeless (TIM). PER and TIM negatively regulate their own expression, closing the loop[5,6]. This circuit can be disrupted by many mutations[23]. Two mutants, $per^{01}$ and $Clk^{Jrk}$, are behaviourally arrhythmic, and show non-cycling expression of circadian components, including PER and TIM[24,25]. To examine peroxiredoxin oxidation patterns in these mutants, they were entrained as described above for wild-type (Canton-S) flies. We observed two circadian cycles of PRX-$SO_{2/3}$ oscillation, with an altered circadian phase relative to wild type. This indicates the presence of an underlying capacity for circadian timing in both mutant strains, which was clearly perturbed by the absence of functional transcriptional feedback circuitry (Fig. 4a).

To establish the wider relevance of these findings, we also examined similar mutants in the fungus *Neurospora crassa*. The *frequency* (*frq*) locus encodes a critical element in the TTFL of *Neurospora*, in addition to the Per–Arnt–Sim (PAS)-containing WC transcription factors[26]. In the long-period $frq^7$ mutant[27], peroxiredoxin oxidation rhythms showed a similarly lengthened period, with an altered phase relative to rhythms in FRQ protein abundance (Fig. 4b). Deletion of the *frq* locus characterizes the $frq^{10}$ strain, and measurable markers of clock output, such as its spore-forming ('conidiation') rhythm, are profoundly perturbed in these fungi, although apparently stochastic oscillations can re-emerge under various growth conditions[27–29]. Circadian rhythms of peroxiredoxin oxidation were, however, clearly seen in $frq^{10}$ mutants sampled in constant darkness (Fig. 4b), with a delayed phase relative to wild-type (*bd*) fungi. This illustrates that peroxiredoxin rhythms represent an alternative readout for an oscillator that persists in the absence of a FRQ-dependent clock.

We next examined the phenotypes of mutant circadian transcriptional regulators in photosynthetic eukaryotes and prokaryotes. The transcriptional clockwork of the plant *Arabidopsis thaliana* and the alga *Ostreococcus tauri* are very similar and rely on circadian oscillation of TOC1. Accordingly, overexpressing *TOC1* in either species disrupts transcriptional rhythms[30,31]. In such strains, under constant light, we observed persistent oscillations of peroxiredoxin oxidation, albeit with altered amplitude and phase relative to controls (Supplementary Figs 2 and 3). Furthermore, in cyanobacteria we assayed peroxiredoxin oxidation in the arrhythmic *KaiA* deletion strain, AMC702 (ref. 32). Notably, an approximately 24-h rhythm of peroxiredoxin oxidation persisted despite a functional Kai-based oscillator being absent, again in an altered phase relative to wild type (Fig. 5a). Taken together, these observations indicate that metabolic rhythms remain closely aligned to transcriptional feedback mechanisms when those mechanisms are present. Crucially, however, metabolic rhythms persist even when cycling clock gene transcription is abolished (summarized in Supplementary Table 9).

Having determined the TTFL influence on peroxiredoxin oxidation rhythms, we reciprocally tested whether rhythmic peroxiredoxin oxidation is required for timekeeping, using TTFL components as markers of the clockwork. We assayed reporter bioluminescence and delayed fluorescence in mutant *S. elongatus* and *A. thaliana* lines, respectively, that were deficient in 2-CysPRX (*Synechococcus* Δ2-CysPRX, GenBank accession AAP49028; *Arabidopsis* double mutant: Δ2-CysPRXA Δ2-CysPRXB, GenBank accessions NM_111995 and NM_120712)[33]. In these mutants, circadian rhythms persisted with wild-type period, albeit significantly perturbed in either phase or amplitude, relative to controls (Fig. 5b and Supplementary Fig. 9). This suggests that peroxiredoxins are not required for oscillator



©2012 Macmillan Publishers Limited. All rights reserved

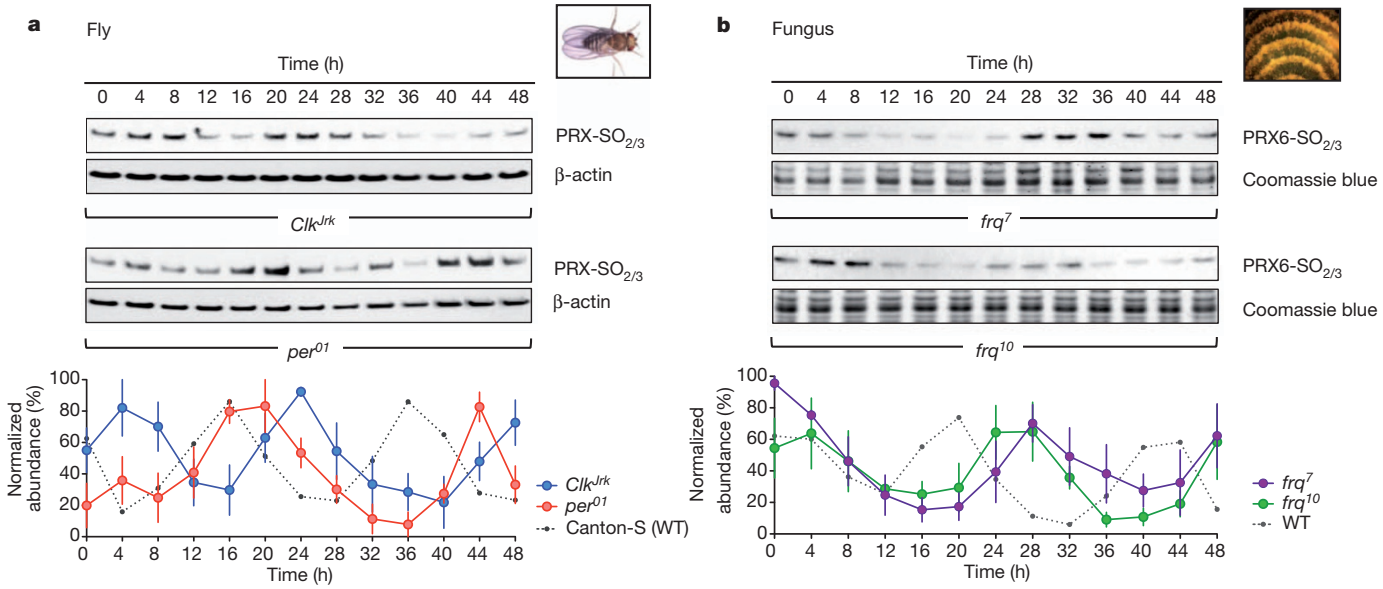


**Figure 4 | Peroxiredoxin oxidation cycles in circadian clock mutants.** **a**, **b**, Representative immunoblots probed for oxidized/hyperoxidized peroxiredoxin (PRX-$SO_{2/3}$ or PRX6-$SO_{2/3}$) are shown for fruitfly (*D. melanogaster*; **a**) and fungus (*N. crassa*; **b**). For each model system, organisms were sampled under free-running conditions (constant darkness). Loading controls show either β-actin immunoblots or Coomassie blue-stained gels loaded with identical samples used for immunoblotting. Immunoblot quantification by densitometry is shown below each panel (mean ± s.e.m.) for $n = 3$ biological replicates. See Supplementary Table 9 for cycle period estimates (by harmonic regression) and detailed statistics (by ANOVA), as well as Supplementary Fig. 10 for TIM and FRQ immunoblots for fruitfly and fungus, respectively. WT, wild type.

function in systems that possess an alternative timing mechanism, namely a TTFL. On the other hand, our findings in TTFL mutants reveal that cellular components that are required for rhythmic outputs are not essential to rhythms in redox metabolism. Given the information that we have about the above model organisms, used commonly to study clock biology, we suggest that both peroxiredoxin and TTFL components of the circadian system are important, but potentially individually dispensable for circadian rhythms at the cellular level. Moreover, the phenotypes of these mutants suggest that the cellular ROS balance is important for robust clock function, as was described recently in *Neurospora*[34].

## Implications for clock evolution

We have observed ~24 h cycles of peroxiredoxin oxidation–reduction in all domains of life and consequently, the possibility that cellular rhythms share a common molecular origin seems increasingly plausible. Because the cellular role of peroxiredoxins principally involves the removal of toxic metabolic by-products (that is, ROS), we proposed that the ability to survive cycles of oxidative stress may have contributed a selective advantage from the beginnings of aerobic life.

Approximately 2.5 billion years ago, photosynthetic bacteria acquired the capacity for photo-dissociation of water, leading to the geologically rapid accumulation of molecular oxygen during the Great Oxidation Event (GOE), when anaerobic life underwent a catastrophic decline[35]. Evidently, organisms that survived the transition to an aerobic environment were those that respired and/or evolved oxygen. As electron transport chains involving oxygen inevitably produce toxic superoxide anions as by-products[36], during the GOE, successful organisms had to acquire ROS removal systems or were relegated to anaerobic niches[35]. Superoxide dismutase, which converts superoxide to hydrogen peroxide, is ubiquitous and, like peroxiredoxin (the major cellular $H_2O_2$ 'sink'), is estimated to have arisen around the time of the GOE[37], the same era during which the most ancient known clock mechanism (the Kai oscillator) evolved. Importantly, we note that (1) during the GOE, rhythms of $O_2$ production/consumption and ROS generation would have been driven by the solar cycle, as they are today[38–40]; (2) metabolic/oxidation rhythms seem to be present in every organism with a circadian clock, all of which are aerobes, and these rhythms persist in the absence of transcriptional cycles; and (3) circadian timekeeping confers a selective advantage when it facilitates anticipation of environmental change (noxious or otherwise).

We believe that the most reasonable interpretation is that cellular metabolism in the most competitive early aerobes adapted to confer anticipation of, and resonate with, environmental cycles in energy supply and oxidative stress. We presume that the echoes of this ancient evolutionary adaptation are revealed by the conserved peroxiredoxin oxidation cycles we now observe in disparate organisms, indicating that during the past 2.5 billion years, ROS and metabolic pathways must have co-evolved with the cellular clockwork, and are probably interlinked. On top of this, further cellular mechanisms seem to have been incorporated, when advantageous, as they arose over time. For example, in eukaryotes, the timekeeping contribution made by certain post-translational mechanisms (such as casein kinase) is conserved across several disparate organisms, whereas clock gene transcription factors are widely divergent, having evolved and been introduced more recently (see Fig. 6).

If there was considerable pressure for the co-evolution of metabolic/ROS pathways with cellular timekeeping systems, then evidence for this should exist in the phylogenetic trees of their component mechanisms. To substantiate this we used the Mirrortree algorithm[41] to assess the degree of co-evolution between the 2-Cys peroxiredoxin family, representing metabolism/ROS pathways, with the most ancient characterized clock mechanism: the three cyanobacterial Kai proteins. Because the Kai proteins are found exclusively in prokaryotes, we focused on these for our analysis[18]. All three components of the cyanobacterial oscillator seem to have co-evolved with 2-Cys peroxiredoxins, as shown by the strong correlation between the distances of respective proteins within each phylogenetic tree (KaiA, $r = 0.784$; KaiB, $r = 0.883$; KaiC, $r = 0.865$; $P < 1 \times 10^{-6}$ for all) (Fig. 5c and Supplementary Fig. 4). Notably, when evolution of KaiC (the most ancient member) was compared with other absolutely conserved protein families, the three highest correlations observed were for the other two clock components (KaiA and KaiB) and for



©2012 Macmillan Publishers Limited. All rights reserved

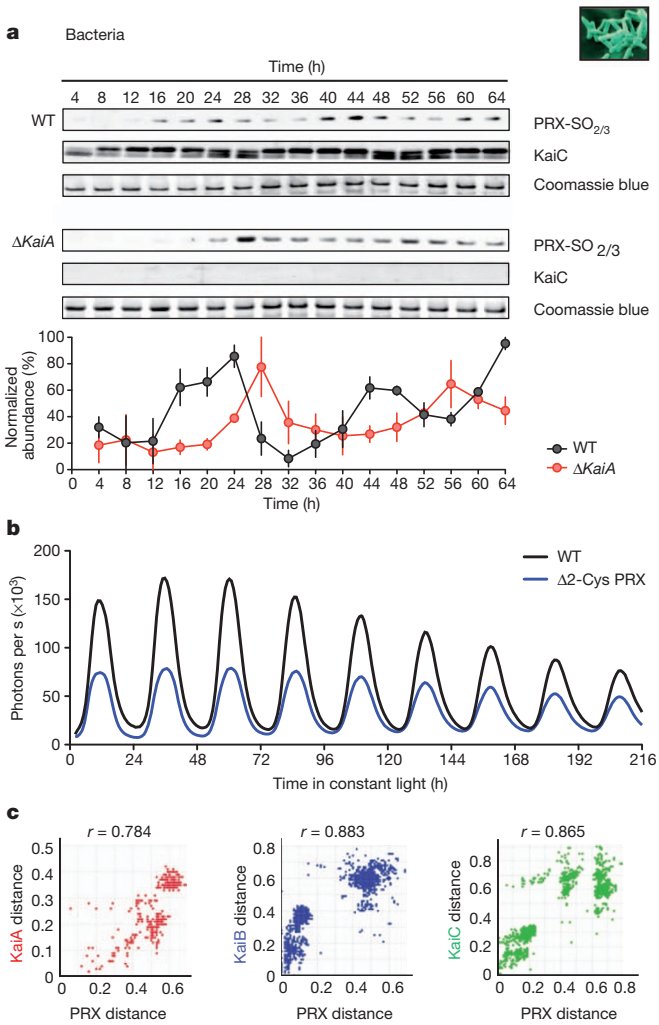


**Figure 5 | Relationships between peroxiredoxins and the cyanobacterial Kai-based oscillator.** **a**, Representative immunoblots for oxidized/hyperoxidized 2-Cys peroxiredoxin (PRX-$SO_{2/3}$) are shown for wild-type (strain AMC149) and KaiA deletion mutant (Δ*KaiA*; strain AMC702) cyanobacteria. Immunoblot quantification by densitometry is shown below each panel (mean ± s.e.m.), $n = 3$ biological replicates. See Supplementary Table 9 for detailed analysis. **b**, Bioluminescence traces for cyanobacteria cultures of wild-type or 2-Cys peroxiredoxin knockout (Δ2-Cys PRX) strains, as reported by *psbAI*p::*luxAB*[49]. **c**, Co-evolution of cyanobacteria oscillator components and peroxiredoxin proteins. Interspecies plots correlate the interprotein distances between Kai proteins and 2-Cys peroxiredoxin[41,50]. *r* denotes the correlation coefficient ($P < 1 \times 10^{-6}$). See Supplementary Table 8 and Supplementary Figs 4–6 for details.

peroxiredoxin (Supplementary Fig. 5 and Supplementary Table 8). This suggests that similarities in the evolutionary profiles of these cellular mechanisms go beyond those that would be expected simply based on the time since a common ancestry, because even highly conserved proteins had considerably inferior correlations to peroxiredoxin (Supplementary Fig. 6 and Supplementary Table 8)[42]. Given that Kai proteins are not found in eukaryotic systems, but metabolic rhythms such as those observed in peroxiredoxin oxidation are, our results suggest that metabolic rhythms are at least as ancient as, and pre-date most, phylum-specific timekeeping mechanisms, but are intrinsically integrated with them in modern organisms.

## Concluding remarks

It has long been recognized that oxygen-sensing PAS-domain proteins are involved in the clockwork of many eukaryotes, but the rationale behind this has remained elusive[23,43–45]. In light of our current findings,

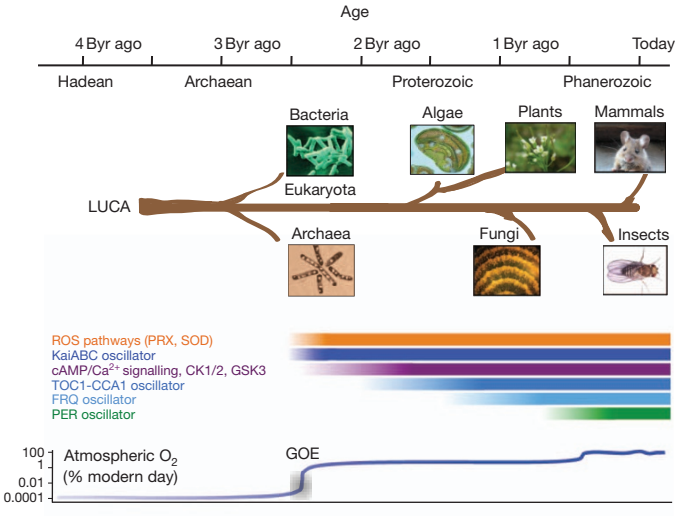


**Figure 6 | Phylogenetic origins of circadian oscillatory systems.** A timeline is shown at the top of the schematic, with the geological era illustrated. A schematic phylogenetic tree shows the origins of each organism studied, stemming from the last universal common ancestor (LUCA). The putative epoch over which each oscillator system has existed is illustrated by the labelled bars. CK1/2, casein kinase 1 or 2; GSK3, glycogen synthase kinase 3; SOD, superoxide dismutase.

we speculate that sensing and responding to oxidative cycles in cellular environments could have driven the evolution of circadian rhythms, and maintained the intrinsic link between clocks and metabolism (Fig. 6). A direct prediction therefore, is that organisms that lack ROS detoxification systems will not have circadian rhythms. At least one such class of organism exists on Earth, an example being the hyperthermophilic archaea *Methanopyri* (NCBI taxonomy accession 183988). Given its distinct anoxic environmental niche and methanogenic metabolism[46], there may never have been a selective evolutionary pressure to develop circadian timekeeping as we know it.

## METHODS SUMMARY

**Organisms and strains.** *A. thaliana*, *D. melanogaster*, *H. salinarum* sp. NRC-1, *M. musculus*, *N. crassa*, *O. tauri* and *S. elongatus* were bred, grown or cultured in appropriate conditions, synchronized by specific methods normally used in each organisms, and then sampled under constant conditions of either darkness or light, depending on the organism.

**Gel electrophoresis and western blotting.** Samples were lysed in LDS buffer and heated to 70 °C for 10 min with constant shaking (600 r.p.m.) in a thermomixer. Electrophoresis was performed using pre-fabricated 4–12% Bis-Tris gradient gels, using a non-reducing MES SDS buffer system, allowing characterization of proteins between 10 and 260 kDa. Immunoblotting was performed after protein transfer to nitrocellulose membranes. After blocking, membranes were incubated in antibody diluted in blocking buffer (0.5% milk in BSA) overnight at 4 °C. The next day, membranes were washed and bands visualized with chemiluminescence detection.

**Phylogenetic analyses.** We used the Mirrortree online server, using input FASTA sequences for human PRDX2 (GenBank accession CAG46588.1) and compared this serially with *S. elongatus* sp. PCC7942 proteins: KaiA (GenBank accession AAM82684.1), KaiB (AAM82685.1) and KaiC (AAM82686.1). Similar analyses were performed for KaiC comparisons with other conserved bacterial proteins. Interspecies plots were generated, which contain a simplified representation of the correlation between the interprotein distances in phylogenetic trees for each protein being compared.

**Image and statistical analysis.** Coomassie-stained gel images were obtained using a Licor Odyssey system, and immunoblot films were scanned using a flat-bed scanner. Densitometric quantification of images was performed using NIH ImageJ software. Signal was normalized against the respective loading control for each replicate at each time point for grouped data. Sine curve fitting was performed using Circwave software, using a harmonic regression method, and analysis of variance (ANOVA) was also performed as an independent measure of temporal variation. Statistical comparisons between Mirrortree correlation coefficients were performed as detailed above.



©2012 Macmillan Publishers Limited. All rights reserved

**Full Methods** and any associated references are available in the online version of the paper at www.nature.com/nature.

**Received 22 July 2011; accepted 26 March 2012.**
**Published online 16 May 2012.**

1. Dunlap, J. C. Molecular bases for circadian clocks. *Cell* **96,** 271–290 (1999).
2. Woelfle, M. A., Ouyang, Y., Phanvijhitsiri, K. & Johnson, C. H. The adaptive value of circadian clocks; an experimental assessment in cyanobacteria. *Curr. Biol.* **14,** 1481–1486 (2004).
3. Dodd, A. N. *et al.* Plant circadian clocks increase photosynthesis, growth, survival, and competitive advantage. *Science* **309,** 630–633 (2005).
4. Barger, L. K., Lockley, S. W., Rajaratnam, S. M. & Landrigan, C. P. Neurobehavioral, health, and safety consequences associated with shift work in safety-sensitive professions. *Curr. Neurol. Neurosci. Rep.* **9,** 155–164 (2009).
5. Wijnen, H. & Young, M. W. Interplay of circadian clocks and metabolic rhythms. *Annu. Rev. Genet.* **40,** 409–448 (2006).
6. Allada, R., Emery, P., Takahashi, J. S. & Rosbash, M. Stopping time: the genetics of fly and mouse circadian clocks. *Annu. Rev. Neurosci.* **24,** 1091–1119 (2001).
7. Rosbash, M. The implications of multiple circadian clock origins. *PLoS Biol.* **7,** e62 (2009).
8. Zheng, X. & Sehgal, A. Probing the relative importance of molecular oscillations in the circadian clock. *Genetics* **178,** 1147–1155 (2008).
9. O'Neill, J. S. *et al.* Circadian rhythms persist without transcription in a eukaryote. *Nature* **469,** 554–558 (2011).
10. O'Neill, J. S. & Reddy, A. B. Circadian clocks in human red blood cells. *Nature* **469,** 498–503 (2011).
11. Hall, A., Karplus, P. A. & Poole, L. B. Typical 2-Cys peroxiredoxins–structures, mechanisms and functions. *FEBS J.* **276,** 2469–2477 (2009).
12. Wood, Z. A., Poole, L. B. & Karplus, P. A. Peroxiredoxin evolution and the regulation of hydrogen peroxide signaling. *Science* **300,** 650–653 (2003).
13. Barranco-Medina, S., Lazaro, J. J. & Dietz, K. J. The oligomeric conformation of peroxiredoxins links redox state to function. *FEBS Lett.* **583,** 1809–1816 (2009).
14. Woo, H. A. *et al.* Reversible oxidation of the active site cysteine of peroxiredoxins to cysteine sulfinic acid. Immunoblot detection with antibodies specific for the hyperoxidized cysteine-containing sequence. *J. Biol. Chem.* **278,** 47361–47364 (2003).
15. Lopez-Molina, L., Conquet, F., Dubois-Dauphin, M. & Schibler, U. The DBP gene is expressed according to a circadian rhythm in the suprachiasmatic nucleus and influences circadian behavior. *EMBO J.* **16,** 6762–6771 (1997).
16. Johnson, C. H., Mori, T. & Xu, Y. A cyanobacterial circadian clockwork. *Curr. Biol.* **18,** R816–R825 (2008).
17. Nakajima, M. *et al.* Reconstitution of circadian oscillation of cyanobacterial KaiC phosphorylation *in vitro*. *Science* **308,** 414–415 (2005).
18. Dvornyk, V., Vinogradova, O. & Nevo, E. Origin and evolution of circadian clock genes in prokaryotes. *Proc. Natl Acad. Sci. USA* **100,** 2495–2500 (2003).
19. Whitehead, K., Pan, M., Masumura, K., Bonneau, R. & Baliga, N. S. Diurnally entrained anticipatory behavior in archaea. *PLoS ONE* **4,** e5485 (2009).
20. Lakin-Thomas, P. L. Transcriptional feedback oscillators: maybe, maybe not. *J. Biol. Rhythms* **21,** 83–92 (2006).
21. Reddy, A. B. & O'Neill, J. S. Healthy clocks, healthy body, healthy mind. *Trends Cell Biol.* **20,** 36–44 (2009).
22. Young, M. W. & Kay, S. A. Time zones: a comparative genetics of circadian clocks. *Nature Rev. Genet.* **2,** 702–715 (2001).
23. Young, M. W. The molecular control of circadian behavioral rhythms and their entrainment in *Drosophila*. *Annu. Rev. Biochem.* **67,** 135–152 (1998).
24. Allada, R., White, N. E., So, W. V., Hall, J. C. & Rosbash, M. A mutant *Drosophila* homolog of mammalian *clock* disrupts circadian rhythms and transcription of *period* and *timeless*. *Cell* **93,** 791–804 (1998).
25. Hardin, P. E. The circadian timekeeping system of *Drosophila*. *Curr. Biol.* **15,** R714–R722 (2005).
26. Dunlap, J. C. & Loros, J. J. How fungi keep time: circadian system in Neurospora and other fungi. *Curr. Opin. Microbiol.* **9,** 579–587 (2006).
27. Aronson, B. D., Johnson, K. A., Loros, J. J. & Dunlap, J. C. Negative feedback defining a circadian clock: autoregulation of the clock gene *frequency*. *Science* **263,** 1578–1584 (1994).
28. Granshaw, T., Tsukamoto, M. & Brody, S. Circadian rhythms in *Neurospora crassa*: farnesol or geraniol allow expression of rhythmicity in the otherwise arrhythmic strains $frq^{10}$, *wc-1*, and *wc-2*. *J. Biol. Rhythms* **18,** 287–296 (2003).
29. Lakin-Thomas, P. L. & Brody, S. Circadian rhythms in microorganisms: new complexities. *Annu. Rev. Microbiol.* **58,** 489–519 (2004).
30. Corellou, F. *et al.* Clocks in the green lineage: comparative functional analysis of the circadian architecture of the picoeukaryote ostreococcus. *Plant Cell* **21,** 3436–3449 (2009).
31. Mas, P., Alabadi, D., Yanovsky, M. J., Oyama, T. & Kay, S. A. Dual role of TOC1 in the control of circadian and photomorphogenic responses in *Arabidopsis*. *Plant Cell* **15,** 223–236 (2003).
32. Ditty, J. L., Canales, S. R., Anderson, B. E., Williams, S. B. & Golden, S. S. Stability of the *Synechococcus elongatus* PCC 7942 circadian clock under directed anti-phase expression of the kai genes. *Microbiology* **151,** 2605–2613 (2005).
33. Pulido, P. *et al.* Functional analysis of the pathways for 2-Cys peroxiredoxin reduction in *Arabidopsis* thaliana chloroplasts. *J. Exp. Bot.* **61,** 4043–4054 (2010).
34. Yoshida, Y., Iigusa, H., Wang, N. & Hasunuma, K. Cross-talk between the cellular redox state and the circadian system in *Neurospora*. *PLoS ONE* **6,** e28227 (2011).
35. Wang, M. *et al.* A universal molecular clock of protein folds and its power in tracing the early history of aerobic metabolism and planet oxygenation. *Mol. Biol. Evol.* **28,** 567–582 (2011).
36. Nathan, C. & Ding, A. SnapShot: reactive oxygen intermediates (ROI). *Cell* **140,** 951–951.e2 (2010).
37. Zelko, I. N., Mariani, T. J. & Folz, R. J. Superoxide dismutase multigene family: a comparison of the CuZn-SOD (SOD1), Mn-SOD (SOD2), and EC-SOD (SOD3) gene structures, evolution, and expression. *Free Radic. Biol. Med.* **33,** 337–349 (2002).
38. Mulholland, P. J., Houser, J. N. & Maloney, K. O. Stream diurnal dissolved oxygen profiles as indicators of in-stream metabolism and disturbance effects: Fort Benning as a case study. *Ecol. Indic.* **5,** 243–252 (2005).
39. Venkiteswaran, J. J., Wassenaar, L. I. & Schiff, S. L. Dynamics of dissolved oxygen isotopic ratios: a transient model to quantify primary production, community respiration, and air-water exchange in aquatic ecosystems. *Oecologia* **153,** 385–398 (2007).
40. Bamforth, S. S. Diurnal changes in shallow aquatic habitats. *Limnol. Oceanogr.* **7,** 348–353 (1962).
41. Ochoa, D. & Pazos, F. Studying the co-evolution of protein families with the Mirrortree web server. *Bioinformatics* **26,** 1370–1371 (2010).
42. Peixoto, A. A., Campesan, S., Costa, R. & Kyriacou, C. P. Molecular evolution of a repetitive region within the *per* gene of *Drosophila*. *Mol. Biol. Evol.* **10,** 127–139 (1993).
43. McIntosh, B. E., Hogenesch, J. B. & Bradfield, C. A. Mammalian Per-Arnt-Sim proteins in environmental adaptation. *Annu. Rev. Physiol.* **72,** 625–645 (2010).
44. Rutter, J., Reick, M. & McKnight, S. L. Metabolism and the control of circadian rhythms. *Annu. Rev. Biochem.* **71,** 307–331 (2002).
45. Rutter, J., Reick, M., Wu, L. C. & McKnight, S. L. Regulation of clock and NPAS2 DNA binding by the redox state of NAD cofactors. *Science* **293,** 510–514 (2001).
46. Shima, S., Thauer, R. K. & Ermler, U. Hyperthermophilic and salt-dependent formyltransferase from *Methanopyrus kandleri*. *Biochem. Soc. Trans.* **32,** 269–272 (2004).
47. Declercq, J. P. *et al.* Crystal structure of human peroxiredoxin 5, a novel type of mammalian peroxiredoxin at 1.5 Å resolution. *J. Mol. Biol.* **311,** 751–759 (2001).
48. Schröder, E. *et al.* Crystal structure of decameric 2-Cys peroxiredoxin from human erythrocytes at 1.7 Å resolution. *Structure* **8,** 605–615 (2000).
49. Xu, Y., Mori, T. & Johnson, C. H. Cyanobacterial circadian clockwork: roles of KaiA, KaiB and the *kaiBC* promoter in regulating KaiC. *EMBO J.* **22,** 2117–2126 (2003).
50. Pazos, F. & Valencia, A. Similarity of phylogenetic trees as indicator of protein-protein interaction. *Protein Eng.* **14,** 609–614 (2001).

**Supplementary Information** is linked to the online version of the paper at www.nature.com/nature.

**Acknowledgements** This work was primarily supported by the Wellcome Trust (083643/Z/07/Z and 093734/Z/10/Z), the European Research Council (ERC Starting Grant No. 281348, MetaCLOCK), and EMBO Young Investigators Programme, as well as the Medical Research Council Centre for Obesity and Related metabolic Disorders (MRC CORD), and the National Institute for Health Research (NIHR) Cambridge Biomedical Research Centre. C.P.K. and M.H.H. acknowledge European Commission grant EUCLOCK (no. 018741) and Biotechnology and Biological Sciences Research Council (BBSRC) grant BB/C006941/1. SynthSys is funded by BBSRC and Engineering and Physical Sciences Research Council (EPSRC) award BB/D019621 to A.J.M. and others. N.S.B. was supported by ENIGMA, US Department of Energy, under contract no. DE-AC02-05CH11231, and by a grant from the National Institutes of Health (NIH; P50GM076547). C.H.J. was supported by the NIH (R01GM088595, R01GM067152 and R21HL102492). M.M. was supported by the Netherlands Organisation for Scientific Research (NWO; Dutch Science Foundation VICI award and Open Programma) and the University of Groningen (Rosalind Franklin Fellowship Program). We thank M. Jain, G. O'Neill and J. Chambers for discussion about the manuscript, and S. G. Rhee, F. Rouyer and R. Stanewsky for the gifts of antisera.

**Author Contributions** A.B.R. and J.S.O. conceived and designed the experiments, and wrote the manuscript. R.S.E., E.W.G., G.v.O., M.O., X.Q., Y.X., Y.Z., M.P., U.K.V., K.A.F. and E.S.M. performed experiments. M.H.H., N.S.B., C.H.J., M.M., A.J.M. and C.P.K. provided reagents. R.S.E., E.W.G., G.v.O., M.O. and Y.Z. contributed equally to this work.

**Author Information** Reprints and permissions information is available at www.nature.com/reprints. The authors declare no competing financial interests. Readers are welcome to comment on the online version of this article at www.nature.com/nature. Correspondence and requests for materials should be addressed to A.B.R. (areddy@cantab.net) or J.S.O. (jso22@medschl.cam.ac.uk).



©2012 Macmillan Publishers Limited. All rights reserved

## METHODS

***Arabidopsis thaliana.*** Surface-sterilized *A. thaliana* seeds (Ws) were plated on solid medium (1.2% agar plus 0.5× Murashige & Skoog medium (Duchefa Biochemie), pH 5.8), vernalized at 4 °C for 4 days, and grown for 7 days under 12 h light, 12 h dark cycles under cool-white fluorescent tubes (70–100 $\mu Em^{-2} s^{-1}$) at 20 °C before transfer to constant light conditions at Zeitgeber time (ZT) 0. Plantlets were sampled every 4 h for 3 days by snap-freezing 15 seedlings per sample in liquid $N_2$. Tissue was crushed in a Tissue Lyser (Eppendorf) using a 0.32-cm chrome ball (Spheric-Trafalgar), and tissue was thawed in extraction buffer (8 M urea, 300 mM NaCl, 100 mM Tris, pH 7.5, 10 mM EDTA, 4% poly(vinylpolypyrrolidone), 1% NP40 and 2× complete protease inhibitors (Roche)) and incubated on ice for 15 min, vortexing every 2 min before centrifugation at 16,000*g* for 10 min. Supernatants were loaded onto gels after the addition of SDS loading buffer (4% SDS, 20% glycerol, 10% 2-mercaptoethanol, 0.004% bromphenol blue and 0.125 M Tris-HCl, ~pH 6.8) and heating to 100 °C for 5 min. Equal protein loading was confirmed by gel electrophoresis and Coomassie staining of gels loaded with equal volumes of lysate from each time point in each replicate set. Delayed fluorescence was performed as reported previously[51].

***Drosophila melanogaster.*** Canton-S (CS) wild-type flies and congenic $per^{01}$ and $Clk^{Jrk}$ mutants were raised on standard medium at 25 °C in 12 h light, 12 h dark cycles, and their behavioural phenotypes were validated using DAM5 activity monitors (TriKinetics)[52]. Adult male flies were entrained for a further 3 days in light boxes at 25 °C before transfer into constant darkness at 25 °C. Flies were collected over two circadian cycles every 4 h, and their heads were dissociated on dry ice in the light and frozen at −80 °C until use. Protein was extracted from 20 fly heads per time point in CHAPS/urea buffer (8 M urea, 4% (w/w) CHAPS, 5 mM magnesium acetate, 10 mM Tris, pH 8.0) with complete protease inhibitors (Roche)[53]. Samples were ground in a 1.5-ml microfuge tube with a miniature pestle. Protein-adjusted supernatants were loaded onto gels after adding appropriate volumes of 4× LDS loading buffer (Invitrogen) to bring the final concentration to 2×, and then heating to 70 °C for 10 min. Equal protein loading was confirmed by gel electrophoresis and Coomassie staining of gels loaded with equal volumes of lysate from every time point in each replicate set.

***Halobacterium salinarum* sp. NRC-1.** Wild-type *H. salinarum* sp. NRC-1 was cultured from a single colony in complete medium at 37 °C with shaking at 125 r.p.m. (Innova Waterbath, New Brunswick Scientific)[54]. We performed experiments using three different starting colonies or biological replicates. Cells were incubated under entrainment conditions for 5 days (12 h light, 12 h dark cycle; daylight was simulated with full spectrum light at 150 $\mu Em^{-2} s^{-1}$) before sampling. After entrainment, samples (2 ml) were collected every 4 h for 3 days in continuous light, at constant cell density. The cell density was maintained by replacing a fixed volume of the culture with equivalent fresh complete medium (30–80 ml) every 4 h[55]. Absorbance at 600 nm ($A_{600\,nm}$) was recorded at each time point, before dilution, to determine how much medium to add, and also to calculate cell numbers for lysate preparation. As previously described, comparative analysis with a similarly processed control culture discounted any unaccounted perturbations that could have been introduced by this periodic dilution[54]. Cell pellets were collected by centrifugation at 1,600*g* for 2 min, decanted, flash-frozen in liquid $N_2$ and stored at −80 °C until protein extraction. Cell pellets were lysed with 2× denaturing LDS sample buffer (Invitrogen) without reducing agent. Total protein was normalized by the addition of 2× LDS sample buffer on the basis of cell numbers in each sample (determined from $A_{600\,nm}$ measurements). Lysates were then passed through a 27-gauge, 1.27-cm needle by syringing (to reduce viscosity of the samples), before heating to 70 °C for 10 min to fully denature proteins before loading on gels. Equal protein loading was confirmed by gel electrophoresis and Coomassie staining of gels loaded with equal volumes of lysate from every time point in each replicate set.

***Mus musculus.*** All animal experimentation was licensed by the Home Office under the Animals (Scientific Procedures) Act 1986, with Local Ethical Review by the Medical Research Council and the University of Cambridge, UK.

**For free-run liver experiments.** Liver tissue was collected from four adult male C57Bl/6 mice once every 3 h on the second cycle after transfer from 12 h light, 12 h dim red light ('dark') to 12 h dim red light, 12 h dim red light (light, 220 $\mu W\,cm^{-2}$; dim red light, <5 $\mu W\,cm^{-2}$) and immediately frozen and then stored at −80 °C before use. Before sampling, animals were stably entrained to a 12 h light, 12 h dim red light cycle for 3–4 weeks. Lysates were prepared in denaturing 2× LDS sample buffer (Invitrogen) with 1:10 β-mercaptoethanol to a final protein concentration of 2 $\mu g\,\mu l^{-1}$, and heated to 70 °C for 10 min before loading on gels. Ten micrograms of protein per lane was loaded for immunoblotting.

**SCN organotypic slice culture experiments.** Wild-type, ~10-day-old pups on a PER2–LUC (mice expressing a period2–luciferase fusion protein), C57BL/6 genetic background[56] were used for experiments. Brains were removed from pups and sectioned at 300 μm with a McIlwain Tissue Chopper. Slices were sorted and trimmed to contain principally SCN tissue and placed onto a Millipore membrane insert (PICMORG) for culture at 37 °C in 5% $CO_2$ as described previously[57]. Slices were transferred to 1.1 ml HEPES buffered medium with 100 μM beetle luciferin (Promega)[58] in a glass-bottomed Petri dish sealed with a coverslip and vacuum grease. Total bioluminescence was recorded with Hamamatsu photomultiplier tube assemblies housed in a light-tight 37 °C incubator, and recordings were expressed as counts per second integrated over 6-min sample bins[59]. SCN slices were collected 'around the clock' every 4 h according to the phase of the PER2–LUC bioluminescence cycle. Circadian time (CT) 0 was operationally defined as the nadir in bioluminescence signal, and CT12 was taken to be at the peak. Individual SCN slices ($n = 3$ per time point) were immersed in 50 μl 2× LDS sample buffer (Invitrogen), and heated to 70 °C for 10 min before loading on gels. For immunoblotting, 10 μl of lysate per lane was loaded. Equal protein loading was confirmed by gel electrophoresis and Coomassie staining of gels loaded with equal volumes of lysate from each time point in each replicate set.

***Neurospora crassa.*** We used the following strains: wild type (*bd*, *matA* Fungal Genetics Stock Center (FGSC) accession 1858), $frq^{10}$ ($bd;frq^{10}$, *matA* FGSC accession 7490), $frq^{7}$ ($bd;frq^{7}$, *matA* FGSC accession 4898) and PRX-KO (NCU06031, *matA* FGSC accession 20012). All strains were maintained on Vogel's minimal media with 1.5% sucrose as a carbon source. Strain manipulation and growth media followed standard procedures[60]. For circadian experiments, cultures were initiated by inoculating $10^6$ conidia in 25 ml of Vogel's medium containing 2% glucose, 0.5% arginine, 10 $ng\,ml^{-1}$ biotin and 0.2% Tween 80. Plates were incubated under constant light for 36 h at 30 °C. Disks (1.2-cm diameter) were cut from the cohesive mycelial pad and three disks were placed in each of a series of 50 ml tubes (or 100 ml flasks) containing 30 ml (or 50 ml) of Vogel's medium with 0.03% glucose, 0.05% arginine and 10 $ng\,ml^{-1}$ biotin[61]. These were incubated at 25 °C under constant light for at least 2 h before staggered transfers to constant darkness (25 °C) with shaking at 150 r.p.m. Mycelia were then collected at 4 h intervals, dried on paper, frozen in liquid $N_2$, and stored at −80 °C. Harvests were consolidated over 8 h to control for development/age of the tissue. All manipulations in the dark were performed under safe red light. For immunoblot analysis, tissue was ground in liquid $N_2$ with a mortar and pestle and suspended in ice-cold extraction buffer (50 mM HEPES, pH 7.4, 137 mM NaCl, 10% glycerol, 5 mM EDTA containing 50 $\mu g\,ml^{-1}$ phenylmethylsulphonylfluoride, 3 $\mu g\,ml^{-1}$ leupeptin and 3 $\mu g\,ml^{-1}$ pepstatin A[62] and a phosphatase inhibitors cocktail (PhosSTOP, Roche)) at a ratio of 0.5 ml of buffer to 0.5 ml of mycelia powder. For immunoblotting, an antiserum directed against human PRX6 (1-Cys) was used[63] (at 1:5,000 dilution) because no typical 2-Cys PRXs are annotated in the *N. crassa* genome so far, and thus antibody specificity could not otherwise be assured. Equal protein loading was confirmed by gel electrophoresis and Coomassie staining of gels loaded with equal volumes of lysate from every time point in each replicate set.

***Ostreococcus tauri.*** *O. tauri* cells were cultured as previously described[9] and entrained in a 12 h light, 12 h dark cycle of blue light (17.5 $\mu Em^{-2} s^{-1}$, Lee lighting filter 724) at a constant temperature of 20 °C. Cultures of the arrhythmic TSL8 line (TOC1-overexpressing) and its parent line CCA1–LUC[30] were transferred into constant light at ZT0 and sampled every 4 h for 3 days. Five microlitres of cells was chilled on ice and pelleted at 4,500*g* at 4 °C for 10 min. The resulting pellet was resuspended in 50 μl sea water[9], and cells were lysed by adding 50 μl 2× extraction buffer (Sigma-Aldrich, LUC-1 kit) and then 100 μl SDS loading buffer (4% SDS, 20% glycerol, 10% 2-mercaptoethanol, 0.004% bromphenol blue and 0.125 M Tris-HCl, ~pH 6.8) while vortexing vigorously. Samples were heated to 100 °C for 5 min to denature proteins before loading on gels. Equal protein loading was confirmed by gel electrophoresis and Coomassie staining of gels loaded with equal volumes of lysate from every time point in each replicate set. For $H_2O_2$ treatment, cells were incubated for 30 min at the stated concentrations diluted in artificial sea water under normal culture conditions before lysis (described earlier).

***Synechococcus elongatus.*** The cyanobacterial strains used were *S. elongatus* sp. PCC7942 wild type (AMC149) and Δ*KaiA* mutant (AMC702). Cells were grown with aeration in constant light of 100 $\mu E\,s^{-1}\,m^{-2}$ at 30 °C to an attenuance (*D*) at 730 nm of 0.3. The $D_{730\,nm}$ was maintained between 0.27 and 0.45 by dilution with fresh BG-11 medium[64,65]. The culture was exposed to 12 h of constant darkness to synchronize the circadian clock, and then returned to constant light. At 4-h intervals under constant light, cells were collected, immediately frozen and then stored at −80 °C. Samples were prepared for immunoblotting as described previously[66]. Equal protein loading was confirmed by gel electrophoresis and Coomassie staining of gels loaded with equal volumes of lysate from every time point in each replicate set. A single knockout for the 2-Cys *S. elongatus* sp. PCC7942 *PRX* gene[67] was generated by inserting an expression cassette for the kanamycin resistance gene into the EcoRI site near the amino-terminal coding region of the gene. For bioluminescence recordings, *psbAI*p::*luxAB* was used

©2012 Macmillan Publishers Limited. All rights reserved

as a reporter, using previously described protocols[68]. The period of all the peroxiredoxin knockout strain showed no significant difference to that of wild-type. For $H_2O_2$ treatment, cells were incubated for 30 min at 1 mM $H_2O_2$ versus vehicle before cell collection.

**Gel electrophoresis and western blotting.** We used NuPAGE Novex 4–12% Bis-Tris gradient gels (Life Technologies), and ran them using the manufacturer's protocol with a non-reducing MES SDS buffer system, allowing characterization of proteins between 10 and 260 kDa[9,10]. Protein transfer to nitrocellulose for blotting was performed using the iBlot system (Life Technologies), with a standard (programme P3, 7 min) protocol. Nitrocellulose was washed briefly, and then blocked for 30 min in 0.5% (w/w) BSA in non-fat dried milk (Marvel) in TBS containing 0.05% Tween-20 (TBST). After three brief washes in TBST, membranes were incubated in antibody diluted in blocking buffer (0.5% milk in BSA) overnight at 4 °C. The next day, membranes were washed in TBST for 5 min three times and then incubated with 1:10,000 horseradish peroxidase (HRP)-conjugated secondary antibody (Sigma-Aldrich) for 30 min. Four more 10-min washes were then performed before performing chemiluminescence detection using Immobilon reagent (Millipore), or ECL Plus reagent (GE Healthcare). To check even protein loading, the gels were stained with Coomassie SimplyBlue (Life Technologies). Antisera against peroxiredoxins were obtained from Abcam and used in blocking buffer ($PRX\text{-}SO_{2/3}$ 1:10,000 dilution, and PRX1 1:2,000). Rabbit anti-Bmal1 antiserum was used at 1:2,000 in 0.5% BSA (Santa Cruz Antibodies). Rabbit anti-PER or anti-TIM was used at 1:10,000 dilution in blocking buffer. Anti-PER and anti-TIM were provided by R. Stanewsky and F. Rouyer, respectively. A mouse monoclonal β-actin antibody (Santa Cruz Antibodies) was used at 1:5,000 in 0.5% milk in BSA. Mouse anti-FRQ antibody was used at a dilution of 1:40 in blocking buffer. Anti-KaiC antiserum was used as described previously[66].

**Phylogenetic analyses.** We used the Mirrortree online server, using input FASTA sequences for human PRDX2 (GenBank accession CAG46588.1) and compared this serially to *S. elongatus* sp. PCC7942 proteins: KaiA (GenBank accession AAM82684.1), KaiB (GenBank accession AAM82685.1) and KaiC (AAM82686.1)[69]. Similar analyses were performed for KaiC comparisons with other conserved bacterial proteins. Interspecies plots were generated, which contain a simplified representation of the correlation between the interprotein distances in phylogenetic trees for each protein being compared[70].

The Mirrortree web server implements the Mirrortree algorithm for calculating the tree similarity between two protein families, which has been demonstrated to be a good predictor of the interaction or functional relationships between them[69,70]. Phylogenetic trees are obtained from these alignments with the neighbour-joining algorithm implemented in ClustalW[70] using bootstrap (100 repetitions) and excluding gaps for the calculation. The distance matrices are obtained by summing the branch lengths that separate each pair of proteins in the tree. Instead of calculating the complete matrices, only the proteins of organisms present in both trees are used. The similarity of trees between the two families is calculated as the correlation between their distance matrices according to the equation:

$$r = \frac{\sum_{i=1}^{n} (R_i - \bar{R})(S_i - \bar{S})}{\sqrt{\sum_{i=1}^{n} (R_i - \bar{R})^2} \sqrt{\sum_{i=1}^{n} (S_i - \bar{S})^2}}$$

in which $n$ is the number of elements of the matrices, that is, $n = (N^2 - N)/2$; $N$ is the number of common organisms; $R_i$ is the element of the first distance matrix; $S_i$ is the corresponding value for the second matrix; and $\bar{R}$ and $\bar{S}$ are the mean values of $R_i$ and $S_i$, respectively. Correlation coefficients obtained for analyses of KaiC distance versus other conserved bacterial proteins (including KaiB, KaiC and PRX2) were compared by converting them to a normally distributed metric using Fisher's $r$-to-$z$ transformation:

$$r' = \frac{1}{2} \ln \left| \frac{1+r}{1-r} \right|$$

in which $r$ is the Mirrortree correlation coefficient; and $r'$ is the Fisher-transformed correlation coefficient. Transformed coefficients ($r'$) were then compared with each other to generate the test statistic, $z$:

$$z = \frac{r'_1 - r'_2}{\sqrt{\frac{1}{N_1 - 3} + \frac{1}{N_2 - 3}}}$$

in which $r'_1$ is the first Fisher-transformed correlation coefficient; $r'_2$ is the second Fisher-transformed correlation coefficient; $N_1$ is number of common organisms in the first correlation; and $N_2$ is number of common organisms in the second correlation. We computed $z$ with $r'_1$ representing the KaiC–PRX2 correlation coefficient, obtaining negative values for higher correlations, and positive values for lower ones (see Supplementary Table 8 and Supplementary Fig. 6). $P$ values were then computed using standard tables (http://faculty.vassar.edu/lowry/rdiff.html).

**Image and statistical analysis.** Coomassie-stained gel images were obtained using a Licor Odyssey system, and immunoblot films were scanned using a back-illuminated flat-bed scanner. Densitometric quantification of images was performed using NIH ImageJ software. Signal was normalized against the respective loading control for each replicate at each time point for grouped data. Sine curve fitting was performed using Circwave software[71], using a harmonic regression method, and ANOVA was also performed as an independent measure of temporal variation. Statistical comparisons between Mirrortree correlation coefficients were performed as detailed earlier.


51. Gould, P. D. *et al.* Delayed fluorescence as a universal tool for the measurement of circadian rhythms in higher plants. *Plant J.* **58,** 893–901 (2009).
52. Rosato, E. & Kyriacou, C. P. Analysis of locomotor activity rhythms in Drosophila. *Nature Protocols* **1,** 559–568 (2006).
53. Reddy, A. B. *et al.* Circadian orchestration of the hepatic proteome. *Curr. Biol.* **16,** 1107–1115 (2006).
54. Whitehead, K., Pan, M., Masumura, K., Bonneau, R. & Baliga, N. S. Diurnally entrained anticipatory behavior in archaea. *PLoS ONE* **4,** e5485 (2009).
55. Mori, T., Binder, B. & Johnson, C. H. Circadian gating of cell division in cyanobacteria growing with average doubling times of less than 24 hours. *Proc. Natl Acad. Sci. USA* **93,** 10183–10188 (1996).
56. Yoo, S. H. *et al.* PERIOD2::LUCIFERASE real-time reporting of circadian dynamics reveals persistent circadian oscillations in mouse peripheral tissues. *Proc. Natl Acad. Sci. USA* **101,** 5339–5346 (2004).
57. House, S. B., Thomas, A., Kusano, K. & Gainer, H. Stationary organotypic cultures of oxytocin and vasopressin magnocellular neurons from rat and mouse hypothalamus. *J. Neuroendocrinol.* **10,** 849–861 (1998).
58. Hastings, M. H., Reddy, A. B., McMahon, D. G. & Maywood, E. S. Analysis of circadian mechanisms in the suprachiasmatic nucleus by transgenesis and biolistic transfection. *Methods Enzymol.* **393,** 579–592 (2005).
59. Maywood, E. S. *et al.* Synchronization and maintenance of timekeeping in suprachiasmatic circadian clock cells by neuropeptidergic signaling. *Curr. Biol.* **16,** 599–605 (2006).
60. Davis, R. H. *Neurospora: Contributions of a Model Organism* (Oxford Univ. Press, 2000).
61. Merrow, M., Brunner, M. & Roenneberg, T. Assignment of circadian function for the *Neurospora* clock gene frequency. *Nature* **399,** 584–586 (1999).
62. Olmedo, M. *et al.* A role in the regulation of transcription by light for RCO-1 and RCM-1, the *Neurospora* homologs of the yeast Tup1–Ssn6 repressor. *Fungal Genet. Biol.* **47,** 939–952 (2010).
63. Woo, H. A. & Rhee, S. G. in *Methods in Redox Signaling* (ed. Das, D.) Ch. 4 19–23 (Mary Ann Liebert, 2010).
64. Ishiura, M. *et al.* Expression of a gene cluster *kaiABC* as a circadian feedback process in cyanobacteria. *Science* **281,** 1519–1523 (1998).
65. Qin, X. *et al.* Intermolecular associations determine the dynamics of the circadian KaiABC oscillator. *Proc. Natl Acad. Sci. USA* **107,** 14805–14810 (2010).
66. Xu, Y. *et al.* Intramolecular regulation of phosphorylation status of the circadian clock protein KaiC. *PLoS ONE* **4,** e7509 (2009).
67. Stork, T., Laxa, M., Dietz, M. S. & Dietz, K. J. Functional characterisation of the peroxiredoxin gene family members of *Synechococcus elongatus* PCC 7942. *Arch. Microbiol.* **191,** 141–151 (2009).
68. Xu, Y., Mori, T. & Johnson, C. H. Cyanobacterial circadian clockwork: roles of KaiA, KaiB and the *kaiBC* promoter in regulating KaiC. *EMBO J.* **22,** 2117–2126 (2003).
69. Ochoa, D. & Pazos, F. Studying the co-evolution of protein families with the Mirrortree web server. *Bioinformatics* **26,** 1370–1371 (2010).
70. Pazos, F. & Valencia, A. Similarity of phylogenetic trees as indicator of protein–protein interaction. *Protein Eng.* **14,** 609–614 (2001).
71. Oster, H., Damerow, S., Hut, R. A. & Eichele, G. Transcriptional profiling in the adrenal gland reveals circadian regulation of hormone biosynthesis genes and nucleosome assembly genes. *J. Biol. Rhythms* **21,** 350–361 (2006).


©2012 Macmillan Publishers Limited. All rights reserved

CORRIGENDUM

doi:10.1038/nature11427

# Corrigendum: Peroxiredoxins are conserved markers of circadian rhythms

Rachel S. Edgar*, Edward W. Green*, Yuwei Zhao*, Gerben van Ooijen*, Maria Olmedo*, Ximing Qin, Yao Xu, Min Pan, Utham K. Valekunja, Kevin A. Feeney, Elizabeth S. Maywood, Michael H. Hastings, Nitin S. Baliga, Martha Merrow, Andrew J. Millar, Carl H. Johnson, Charalambos P. Kyriacou, John S. O'Neill & Akhilesh B. Reddy

*Nature* **485,** 459–464 (2012); doi:10.1038/nature11088

In the author list of this Article, the names of Gerben van Ooijen and Maria Olmedo should also have been asterisked, indicating their equal contributions. This error has been corrected in the HTML and PDF versions of the original paper.

*These authors contributed equally to this work.



©2012 Macmillan Publishers Limited. All rights reserved